

# A Quantitative Estimation of the Transport of Surface Emissions from Different Regions into the Stratosphere

Fei Xie<sup>1,2</sup>, Jianping Li<sup>1,2</sup>, Wenshou Tian<sup>3</sup>, Dingzhu Hu<sup>4</sup>, Jiankai Zhang<sup>3</sup>,  
Jianchuan Shu<sup>5</sup> and Chunxiao Wang<sup>3</sup>

<sup>1</sup>College of Global Change and Earth System Science, Beijing Normal University, Beijing, China

<sup>2</sup>Joint Center for Global Change Studies, Beijing, China

<sup>3</sup>Key Laboratory for Semi-Arid Climate Change of the Ministry of Education, College of Atmospheric Sciences, Lanzhou University, China

<sup>4</sup>Key Laboratory of Meteorological Disaster of Ministry of Education, Nanjing University of Information Science & Technology, Nanjing, China

<sup>5</sup>Institute of Plateau Meteorology, China Meteorological Administration, Chengdu, China

## Abstract

The transport of chemical compounds from surface emissions into the stratosphere is very important for stratospheric, and even global, climate change. However, the lack of observational data makes it difficult to trace these emissions back to specific regions. This study uses numerical simulations to investigate the transport of surface emissions from high population density regions into the stratosphere. In March, April and May, Southeast Asia and Australia tracers contribute  $\sim\frac{1}{3}$  and  $\sim\frac{1}{4}$  of total tracers entering the stratosphere, respectively. In June, July and August, Southwest Asia contributes  $\sim\frac{1}{2}$  of the total, which is far more than the contribution of all other source regions. In September, October and November, South America and Southeast Asia each accounts for  $\sim\frac{1}{4}$  of the total tracer budget. In December, January and February, Australia and Southeast Asia each accounts for  $\sim\frac{1}{4}$  of all tracers entering the stratosphere. A further quantitative estimation illustrates that the average proportion of a tracer entering the stratosphere compared with its total release is 2.6% for Southeast Asia, followed by 1.7% for Australia, 1.4% for Southwest Asia, 1.0% for Africa, 1.0% for South America, 0.9% for East Asia, 0.7% for North America, and 0.3% for Europe.

(Citation: Xie, F., J. Li, W. Tian, D. Hu, J. Zhang, J. Shu, and C. Wang, 2016: A quantitative estimation of the transport of surface emissions from different regions into the stratosphere. *SOLA*, 12, 65–69, doi:10.2151/sola.2016-015.)

## 1. Introduction

Air in the troposphere contains potent greenhouse gases and active chemical compounds. The transport of tropospheric air masses into the stratosphere potentially affects the stratospheric climate system (Lacis et al. 1992; Gauss et al. 2003; Forster et al. 2007; Solomon et al. 2011). Thus, key questions to be resolved include: How do tropospheric air masses enter the stratosphere? What processes control the transport of tropospheric air into the stratosphere? What proportion of surface emissions from high-density regions reaches the stratosphere?

There has been considerable investigation into how tropospheric air masses enter the stratosphere. Key mechanisms for this in the tropics include deep convection (Fueglistaler et al. 2004; Hosking et al. 2010), Brewer–Dobson (BD) circulation (Holton et al. 1995; Austin and Li 2006; Randel et al. 2007), and tropical cyclones (Cairo et al. 2008; Zhan and Wang 2012). Synoptic scale processes in the mid-latitudes associated with stratosphere and troposphere exchange processes include tropopause folding (Li et al.

2015a, 2015b; Sprenger et al. 2003; Stohl et al. 2003; Pan et al. 2010; 2014) and the Asian summer monsoon (Randel et al. 2010; Bian et al. 2011, 2012; Bourassa et al. 2012). Extreme events such as volcanic explosions also play a role in tropospheric–stratospheric exchange processes (Textor et al. 2003; Vernier et al. 2011). Previous studies have shown that tropospheric compounds and aerosols can be delivered to the stratosphere during stratosphere and troposphere exchange (STE) events (e.g., Rasch et al. 1997; Flocke et al. 1999), and illustrate the importance of understanding key mechanisms for the transport of tropospheric air masses into the stratosphere at the tropopause level (e.g., Levine et al. 2007; Gettelman et al. 2009). Further, the importance of tropospheric air entering the stratosphere through different channels at the tropopause has also been investigated (Skerlak et al. 2014).

Chemical compounds discharged from global different regions can be transported into the stratosphere via STE processes. However, the transport of surface emissions into the tropospheric atmosphere is strongly influenced by many factors, e.g., topography (Fu et al. 2006; Su et al. 2011), convective overshooting (Sun and Huang 2015), and “Tape-recorder” (Liu et al. 2007; Jiang et al. 2015). Because topography and thermal characteristics vary between different regions, the transport of chemical compounds and aerosols horizontally in the troposphere and vertically from the troposphere into the stratosphere is also variable (Jiang et al. 2007; Wang et al. 2014). Obviously, there are many emission sources on the Earth’s surface, but it is unclear what quantity of emissions from each region enters the stratosphere.

East Asia, Southeast Asia, Southwest Asia, Europe, Africa, South America, North America, and Australia represent regions with relatively high concentrations of human life (Fig. 1). According to the current observations, it is difficult to estimate the quantitative contribution of the respective emissions entering stratosphere compared with the total emissions entering stratosphere. In an attempt to better understand the movement of emissions from these sources into the stratosphere, tracers are released simultaneously at the same rate from all regions in the Whole Atmosphere Community Climate Model version 4 (WACCM4). Shu et al. 2010 showed that the WACCM model could effectively and correctly simulate tracer transport in the atmosphere compared with observed mass transport. In this study, WACCM4 is used to estimate the movement of surface emissions into the stratosphere, and then to investigate the respective contributions of these regions to the total emissions that enter the stratosphere. One tracer is released per region; i.e., eight tracers in total. Fig. 1 shows tracer source regions and discharge sites. These eight regions do not include all emission sources on Earth, but basically encompass the primary areas with the highest surface emissions.

## 2. Method, model and experimental design

WACCM4 (Marsh et al. 2013) has 66 vertical levels extending from the ground to  $4.5 \times 10^{-6}$  hPa (ca. 160 km geometric altitude),

Corresponding author: Jianping Li, College of Global Change and Earth System Science, Beijing Normal University, No. 19, Xijiekouwai St., HaiDian District, Beijing 100875, P. R. China. E-mail: lj@bnu.edu.cn. ©2016, the Meteorological Society of Japan.

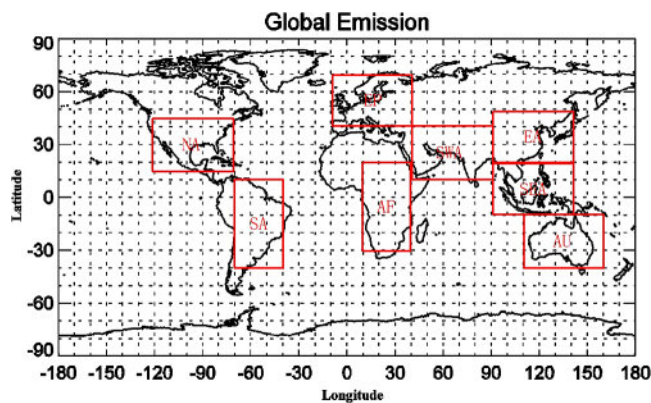


Fig. 1. Eight regional emission sites used in model simulations, denoted AU (Australia), EA (East Asia), SEA (Southeast Asia), SWA (Southwest Asia), EP (Europe), AF (Africa), SA (South America), and NA (North America).

with a vertical resolution of 1.1–1.4 km in the tropical tropopause layer and the lower stratosphere (< 30 km). The simulations presented in this paper were performed at a resolution of  $2.5^\circ \times 1.9^\circ$  (longitude  $\times$  latitude). Observational SST and sea-ice datasets used in the model were obtained from the Meteorological Office, Hadley Centre for Climate Prediction and Research (Rayner et al. 2003). Fixed greenhouse gas (GHG) values used in the model radiation scheme are based on emissions scenario A2 of the Intergovernmental Panel on Climate Change, which uses average GHG values for the period 1980–2010. Quasi-biennial oscillation (QBO) phase signals with a fixed period of 28 months are included in WACCM4 as an external forcing for zonal wind.

The WACCM4 is run for a five-year spin-up period before the tracers are emitted. To investigate tracer transport in the March, April and May (MAM), the eight tracers are discharged on March 1 in the sixth model year and continually discharged for three months. It is E1-MAM (E1 is experiment 1, MAM is the emission time). Because emissions transport varies between seasons, experiments are also performed for June, July and August (E1-JJA), September, October and November (E1-SON), and December, January and February (E1-DJF). The tracers are discharged on June 1, September 1, and December 1, and then continually discharged for three months. A description of the experimental design for all seasons is provided in Table 1. Based on these experiments, it is possible to determine how much of the tracer could transport into the stratosphere during one season emitting of this tracer. To avoid the influence of different QBO phases on model results, three other experiments are also performed in which tracers are discharged during four months of the seventh (E2), eighth (E3) and ninth (E4) model years. The results will be obtained by  $(E1 + E2 + E3 + E4)/4$  which represents the averaged situation.

In this study, the emission quantity of each tracer is same. This study will quantitatively evaluate the proportion of surface emissions from different regions transported into the stratosphere. According to these results, if local emissions are measured, it is possible to evaluate the delivery of local chemical species to the stratosphere. Source region areas in Fig. 1 are calculated according to:  $\text{lat} \times \text{lon} \times \cos\theta$ , where lat is the latitude range, lon is the longitude range and  $\theta$  is the latitude degree of the model column. Each source region has the same latitude and longitude range.

To produce constant emissions quantities in each source region, we set the emission quantity to  $1/\cos\theta$  kg/kg/m<sup>2</sup> in each model column. The total emission quantity of each region can thus be represented as  $1/\cos\theta$  kg/kg/m<sup>2</sup>  $\times$  (lat  $\times$  lon  $\times$  cos $\theta$ ) = lat  $\times$  lon kg/kg/m<sup>2</sup>. Thus, the amount of tracer discharged from each source is the same.

To confirm the validity of tracer release in the model, Fig. 2 shows the spatial distribution of tracer released from the Southeast Asia source region in the MAM experiment, with tracers discharged on March 1. This shows emissions patterns at the surface (1000 hPa), 200 hPa, and 85 hPa, after tracers have been discharged for 2, 5, and 20 days, respectively. The Southeast Asia tracer can't found above 200 hPa only after 2 days have lapsed (Figs. 2a, b, c); on the fifth day, it appears at 200 hPa (Figs. 2d, e, f); and after 20 days, it is found at 85 hPa (Figs. 2g, h, i). Figure 2 illustrates that tracer release and transport is consistent with the basic physical characteristics of atmospheric mass transport. To further ensure the simulated mass transported by WACCM is rational, the simulated vertical transport of CO is compared with observation. Figure 3 shows the CO variations in the stratosphere from 2005 to 2010 from simulation and observation. It is found that the simulated vertical transport of CO (Fig. 3b) is in agreement with that of observation (Fig. 3a).

### 3. Results

To investigate the seasonal contribution of tracers from different source regions to the total entering the stratosphere, Table 2 shows the proportion of a tracer from its region that enters the stratosphere during each 3-month season compared with the total quantity of all tracers entering the stratosphere. In MAM, for the total tracer enters the stratosphere, Southeast Asia accounts for 32.2%, Australia accounts for 17.2%, Southwest Asia is 14.0% and Africa both is 13.6%, East Asia is 8.0%, North America is 6.9%, South America is 5.7%, 2.3% for Europe. In JJA, Southwest Asia accounts for 47.6%, 16.7% for Southeast Asia and 14.2% for East Asia, Africa is 7.0%, Europe is 4.8% and North America each is 4.2%, South America and Australia both are 2.7%. In SON, Southeast Asia, South America, Australia, Southwest Asia, Africa, North America, East Asia and Europe respectively account for 25.6%, 23.1%, 12.8%, 11.0%, 10.7%, 7.7%, 6.4% and 2.6%. In DJF, Southeast Asia is 28.6%, Australia is 24.0%, East Asia and South America each accounts for 9.4%, Africa 8.8%, Southwest Asia is 8.2%, North America is 7.8% and 3.9% for Europe.

Summary of Table 2, in MAM, the Southeast Asia tracer contributes  $\sim 1/3$  of total tracers entering the stratosphere and Australia contributes  $\sim 1/4$ . In JJA, Southwest Asia contributes  $\sim 1/2$  of the total, which is far more than the contribution of all other source regions. It is agree with previous study (Yan and Bian 2015). In SON, Southeast Asia and South America each account for  $\sim 1/4$  of the total tracer budget. In DJF, Southeast Asia and Australia each account for  $\sim 1/4$  of all tracers entering the stratosphere.

To compare the quantities of tracers that enter the stratosphere from different surface sources, Table 3 shows the proportion of a tracer entering the stratosphere compared with its total release from its region during each season. In MAM, 2.8% of the total Southeast Asia tracer enters the stratosphere compared with 1.2%–1.5% for Australia, Southwest Asia, and Africa tracers. For East Asia, Europe, South America, and North America, only 0.2%–0.7% of total tracers reach the stratosphere in the MAM experiment. In JJA, 2% of the total Southwest Asia tracer reaches

Table 1. The experimental design in E1, E2, E3 and E4. Same as E1, except that the tracers discharged in seventh, eighth and ninth model years, respectively

E1-MAM	E1-JJA	E1-SON	E1-DJF
Eight tracers synchronously released at the same rate	Same as E1-MAM	Same as E1-MAM	Same as E1-MAM
Tracers discharged on March 1 in the sixth model year and continually discharged for three months	Same as E1-MAM, but Tracers discharged on June 1	Same as E1-MAM, but Tracers discharged on September 1	Same as E1-MAM, but Tracers discharged on December 1



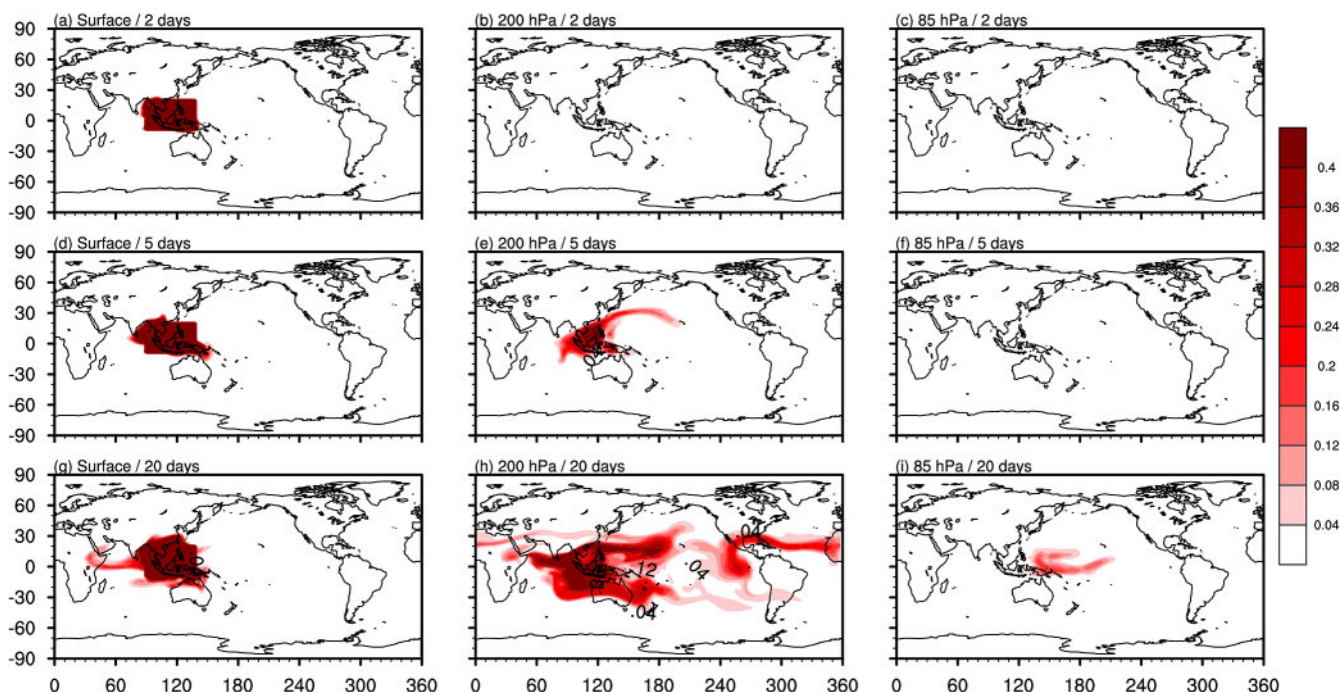


Fig. 2. The spatial distribution of tracers from Southeast Asia (E1-MAM) at the surface after tracers have been discharged for (a) 2 days, (d) 5 days, and (g) 20 days, respectively. (b), (e), and (h) are as above but for 200 hPa; (c), (f), and (i) are as above but for 85 hPa. The contour level is 0.04 kg/kg.

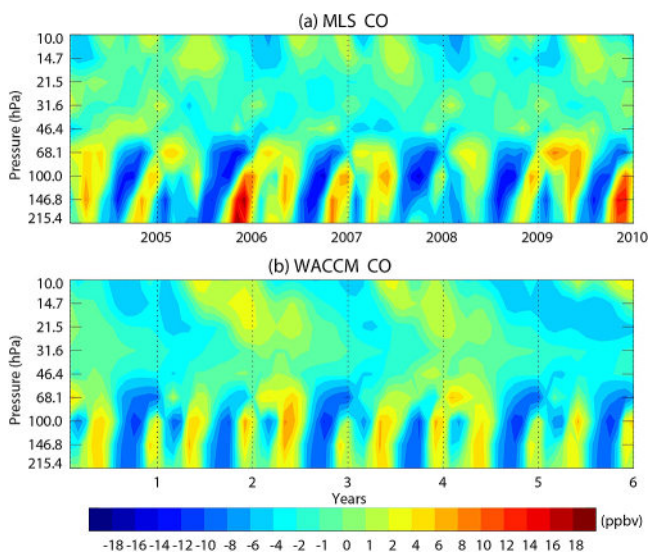


Fig. 3. The (a) MLS and (b) modeled zonal mean CO anomalies averaged over the latitude band 10°N–10°S. The modeled CO anomalies are weighted by MLS averaging kernels. The anomalies here are defined as detrended CO time series with 6yrs mean removed from the original time series. Note that only 6 years of model data are shown since the MLS CO observations cover years from 2005 to 2010.

the stratosphere compared with less than 1% of tracers from all other source regions. In SON, 2% of total Southeast Asia tracer enters the stratosphere compared with 1.0%–1.5% for Australia, Southwest Asia, and South America. For East Asia, Europe, Africa, and North America, less than 1% of total tracers reach the stratosphere in the SON experiment. In DJF, 4.9% of total Southeast Asia tracer and 4.1% of total Australia tracer are transported into the stratosphere. The proportions of tracers entering the stratosphere from other regions are also high (1.4%–1.6%), except for Europe (0.6%).

In Table 3, the rightmost column shows the average percent of

Table 2. The proportion of a tracer from its region that enters the stratosphere during each 3-month season compared with the total quantity of all tracers entering the stratosphere. The results are obtained by  $(E1 + E2 + E3 + E4)/4$ .

	MAM	JJA	SON	DJF
Australia	17.2%	2.7%	12.8%	24.0%
East Asia	8.0%	14.2%	6.4%	9.4%
Southeast Asia	32.2%	16.7%	25.6%	28.6%
Southwest Asia	14.0%	47.6%	11.0%	8.2%
Europe	2.3%	4.8%	2.6%	3.9%
Africa	13.6%	7.0%	10.7%	8.8%
South America	5.7%	2.7%	23.1%	9.4%
North America	6.9%	4.2%	7.7%	7.8%

\* The stratosphere is defined as lapse rate tropopause to 0.1 hPa in the study. Calculation of the tropopause based on the model output’s air temperature.

Table 3. The proportion of a tracer entering the stratosphere compared with its total release from its region during each 3-month season. The rightmost column shows the average percent of a tracer that enters the stratosphere. The lowest line shows the average percent of all tracers entering the stratosphere in 3-month season. The results are obtained by  $(E1 + E2 + E3 + E4)/4$ .

	MAM	JJA	SON	DJF	Average
Australia	1.5%	0.1%	1.0%	4.1%	1.7%
East Asia	0.7%	0.6%	0.5%	1.6%	0.9%
Southeast Asia	2.8%	0.7%	2.0%	4.9%	2.6%
Southwest Asia	1.2%	2.0%	0.9%	1.5%	1.4%
Europe	0.2%	0.2%	0.2%	0.6%	0.3%
Africa	1.2%	0.3%	0.9%	1.5%	1.0%
South America	0.5%	0.1%	1.8%	1.6%	1.0%
North America	0.6%	0.2%	0.6%	1.4%	0.7%
Average	1.1%	0.5%	1.0%	2.1%	

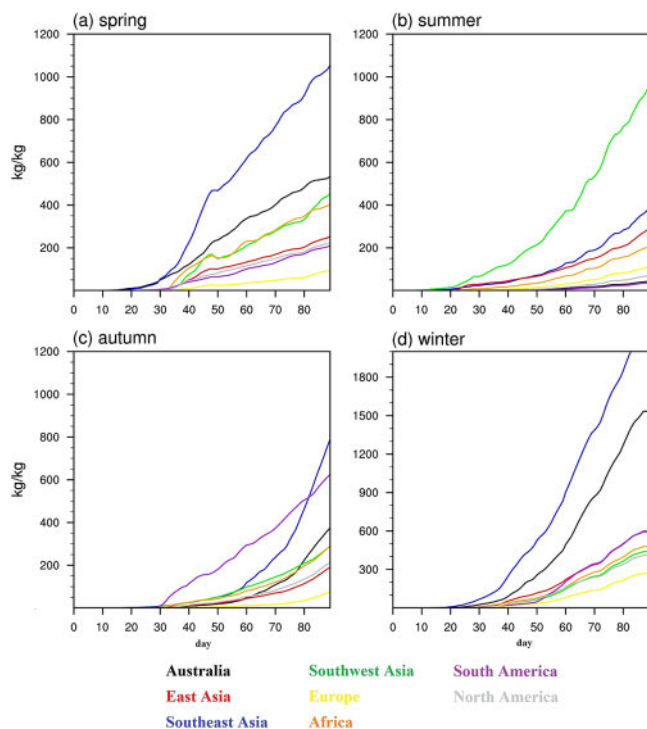


Fig. 4. The variations of total quantity of tracers with time in the stratosphere. (a) spring, (b) summer; (c) autumn; (d) winter. The different colour represents different tracer. Please see the right side of the figure.

a tracer that enters the stratosphere. The highest annual proportion of total tracer that enters the stratosphere is from Southeast Asia (2.6%), followed by Australia (1.7%), Southwest Asia (1.4%), Africa (1.0%), South America (1.0%), East Asia (0.9%), North America (0.7%), and Europe (0.3%). The bottom values in Table 3 shows the average percent of all tracers entering the stratosphere in 3-month season. The quantity of tracers entering stratosphere is highest in DJF (2.1%), followed by MAM (1.1%), SON (1.0%), and JJA (0.5%).

The variations of total quantity of tracers with time in the stratosphere are shown in Fig. 4. It illustrates that, in spring, the tracer from Southeast Asia is the fastest into the stratosphere and the tracer from Europe is the slowest (Fig. 4a). Asia summer monsoon influences the tracer transport in summer. Figure 4b shows that the speed of the tracer from Southwest Asia entering stratosphere is very fast. Tracer from South American has the slowest speed. In the first two months of autumn, the speed of the tracer from South American is much faster than other tracers (Fig. 4c). However, in the third month of autumn, the tracer from Southeast Asia is the fastest entering stratosphere. In winter, the speeds of tracers from Southeast Asia and Australia are very fast (Fig. 4d). The speeds of different tracers coming into stratosphere are corresponding to the results from Tables 2 and 3.

#### 4. Conclusions and discussions

Because tropospheric masses primarily enter the stratosphere over the maritime continent (Sherwood 2000; Sherwood and Dessler 2001; Hosking et al. 2012), the contribution of Southeast Asia emissions to the total entering the stratosphere is very large during all seasons. In JJA, the contributions of Southwest Asia and Southeast Asia are much larger than other regions due to the Asian summer monsoon. A previous study pointed out that tropospheric pollutants transported into the stratosphere by the Asian summer monsoon possibly from China (Hofmann et al. 2009). Our result suggests that the tropospheric pollutants tend to originate from Southwest Asia and Southeast Asia. In SON, it is interesting to

note that the tracer from South America has the same contribution to total stratospheric emissions as that from Southeast Asia. BD circulation is strongest in DJF, which leads to the enhanced delivery of tracers to the stratosphere in DJF compared with other seasons. In DJF (Southern Hemisphere summer), Australia emissions to the stratosphere are comparable with Southeast Asia, and may be associated with the Australian summer monsoon (Li et al. 2012).

It must be pointed out that chemical loss and the physical subsidence of mass are not considered in the simulations. The interactive chemistry is disabled in WACCM4. Thus, the results may overestimate the quantity of very short-lived or heavy species entering the stratosphere.

#### Acknowledgements

This work was jointly supported the National Natural Science Foundation of China (41225018, 41575039, and 41405043). All results reported in the study are from WACCM4 simulations. We thank NCAR for providing the WACCM4 model (<https://www2.cesm.ucar.edu/models/current>).

Edited by: T. Takemi

#### References

- Austin, J., and F. Li, 2006: On the relationship between the strength of the Brewer-Dobson circulation and the age of stratospheric air. *Geophys. Res. Lett.*, **33**, L17807.
- Bian, J., R. Yan, H. Chen, D. Lu, and S. T. Massie, 2011: Formation of the summertime ozone valley over the Tibetan Plateau: The Asian summer monsoon and air column variations. *Adv. Atmos. Sci.*, **28**, 1318–1325.
- Bian, J., L. Pan, L. Paulik, H. Vömel, H. Chen, and D. Lu, 2012: In situ water vapor and ozone measurements in Lhasa and Kunming during the Asian summer monsoon. *Geophys. Res. Lett.*, **39**, L19808.
- Bourassa, A., A. Robock, W. Randel, T. Deshler, L. A. Rieger, N. D. Lloyd, E. J. L. Lewellyn, and D. A. Degenstein, 2012: Large volcanic aerosol load in the stratosphere linked to Asian monsoon transport. *Science*, **337**, 78–81.
- Cairo, F., and co-authors, 2008: Morphology of the tropopause layer and lower stratosphere above a tropical cyclone: A case study on Cyclone Davina 1999. *Atmos. Chem. Phys.*, **8**, 3411–3426.
- Flocke, F., R. L. Herman, R. J. Salawitch, E. Atlas, C. R. Webster, S. M. Schauffler, R. A. Lueb, R. D. May, E. J. Moyer, K. H. Rosenlof, D. C. Scott, D. R. Blake, and T. P. Bui, 1999: An examination of chemistry and transport processes in the tropical lower stratosphere using observations of long-lived and short-lived compounds obtained during STRAT and POLARIS. *J. Geophys. Res.*, **104**, 26625–26642.
- Forster, P., V. Ramaswamy, P. Artaxo, T. Berntsen, R. Betts, D. W. Fahey, J. Haywood, J. Lean, D. C. Lowe, G. Myhre, J. Nganga, R. Prinn, G. Raga, M. Schulz, and R. Van Dorland, 2007: Changes in atmospheric constituents and in radiative forcing. In: *Climate Change 2007: The Physical Science Basis. Contribution of Working Group I to the Fourth Assessment Report of the Intergovernmental Panel on Climate Change* [Solomon, S., D. Qin, M. Manning, Z. Chen, M. Marquis, K. B. Averyt, M. Tignor and H. L. Miller (eds.)]. Cambridge University Press, Cambridge, United Kingdom and New York, NY, US.
- Fu, R., Y. Hu, J. S. Wright, J. H. Jiang, R. E. Dickinson, M. Chen, M. Filipiak, W. G. Read, J. W. Waters, and D. L. Wu, 2006: Short circuit of water vapor and polluted air to the global stratosphere by convective transport over the Tibetan Plateau. *Proc. Nat. Acad. Sci.*, **103**, 5664–5669.
- Fueglistaler, S., H. Wernli, and T. Peter, 2004: Tropical troposphere to stratosphere transport inferred from trajectory

- calculations. *J. Geophys. Res.*, **109**, D03108.
- Gauss, M., and co-authors, 2003: Radiative forcing in the 21st century due to ozone changes in the troposphere and the lower stratosphere. *J. Geophys. Res.*, **108**, 4292.
- Gettelman, A., P. H. Lauritzen, M. Park, and J. E. Kay, 2009: Processes regulating short-lived species in the tropical tropopause layer. *J. Geophys. Res.*, **114**, D13303.
- Holton, J. R., P. H. Haynes, M. E. McIntyre, A. R. Douglass, R. B. Rood, and L. L. Pfister, 1995: Stratosphere-troposphere exchange. *Rev. of Geophys.*, **33**, 403–439.
- Hofmann, D., J. Barnes, M. Neill, M. Trudeau, and R. Neely, 2009: Increase in background stratospheric aerosol observed with LIDAR at Mauna Loa Observatory and Boulder, Colorado. *Geophys. Res. Lett.*, **36**, L15808.
- Hosking, J. S., M. R. Russo, P. Braesicke, and J. A. Pyle, 2010: Modelling deep convection and its impacts on the tropical tropopause layer. *Atmos. Chem. Phys.*, **10**, 11175–11188.
- Hosking, J. S., M. R. Russo, P. Braesicke, and J. A. Pyle, 2012: Tropical convective transport and the Walker circulation. *Atmos. Chem. Phys.*, **12**, 9791–9797.
- Jiang, J. H., N. J. Livesey, H. Su, L. Neary, J. C. McConnell, and N. A. D. Richards, 2007: Connecting surface emissions, convective uplifting, and long-range transport of carbon monoxide in the upper troposphere: New observations from the Aura Microwave Limb Sounder. *Geophys. Res. Lett.*, **34**, L18812.
- Jiang, J. H., H. Su, C. Zhai, L. Wu, K. Minschwaner, A. M. Molod, and A. M. Tompkins, 2015: An assessment of upper-troposphere and lower-stratosphere water vapor in MERRA, MERRA2 and ECMWF reanalyses using Aura MLS observations. *J. Geophys. Res.*, **120**, 11468–11485.
- Lacis, A., J. Hansen, and M. Sato, 1992: Climate forcing by stratospheric aerosols. *Geophys. Res. Lett.*, **19**, 1607–1610.
- Levine, J. G., P. Braesicke, N. R. P. Harris, N. H. Savage, and J. A. Pyle, 2007: Pathways and timescales for troposphere to stratosphere transport via the tropical tropopause layer and their relevance for very short lived substances. *J. Geophys. Res.*, **112**, D04308.
- Li, D., and J. C. Bian, 2015: Observation of a summer tropopause fold by ozonesonde at Changchun, China: Comparison with reanalysis and model simulation. *Adv. Atmos. Sci.*, **32**, 1354–1364.
- Li, D., J. C. Bian, and Q. J. Fan, 2015: A deep stratospheric intrusion associated with an intense cut-off low event over East Asia. *Science China: Earth Sciences*, **58**, 116–128.
- Li, J., J. Feng, and Y. Li, 2012: A possible cause of decreasing summer rainfall in northeast Australia. *Int. J. Climatol.*, **32**, 995–1005.
- Liu, C., E. J. Zipster, T. J. Garrett, J. H. Jiang, and H. Su, 2007: How do the water vapor and carbon monoxide ‘tape recorders’ start near the tropical tropopause. *Geophys. Res. Lett.*, **34**, L09804.
- Marsh, D., M. Mills, D. Kinnison, J. Lamarque, N. Calvo, and L. Polvani, 2013: Climate change from 1850 to 2005 simulated in CESM1 (WACCM). *J. Climate*, **26**, 7372–7391.
- Pan, L. L., and co-authors, 2010: The Stratosphere-Troposphere Analyses of Regional Transport 2008 (START08) Experiment. *Bull. Amer. Meteor. Soc.*, **91**, 327–342.
- Pan, L. L., L. C. Paulik, S. B. Honomichl, L. A. Munchak, J. Bian, H. B. Selkirk, and H. Vömel, 2014: Identification of the tropical tropopause transition layer using the ozone-water vapor relationship. *J. Geophys. Res.*, **119**, 3586–3599.
- Rasch, P. J., N. M. Mahowald, and B. E. Eaton, 1997: Representations of transport, convection, and the hydrologic cycle in chemical transport models: Implications for the modeling of short-lived and soluble species. *J. Geophys. Res.*, **102**, 28127–28138.
- Randel, W. J., M. Park, F. Wu, and N. Livesey, 2007: A large annual cycle in ozone above the tropical tropopause linked to the Brewer–Dobson circulation. *J. Atmos. Sci.*, **64**, 4479–4488.
- Randel, W. J. and co-authors, 2010: Asian monsoon transport of pollution to the stratosphere. *Science*, **328**, 611–633.
- Rayner, N. A., D. E. Parker, E. B. Horton, C. K. Folland, L. V. Alexander, D. P. Rowell, E. C. Kent, and A. Kaplan, 2003: Global analysis of sea surface temperature, sea ice, and night marine air temperature since the late nineteenth century. *J. Geophys. Res.*, **108**, doi:10.1029/2002JD002670.
- Sherwood, S. C., 2000: A stratospheric “drain” over the maritime continent. *Geophys. Res. Lett.*, **27**, 677–680.
- Sherwood, S. C., and A. E. Dessler, 2001: A model for transport across the tropical tropopause. *J. Atmos. Sci.*, **58**, 765–779.
- Shu, J., W. Tian, J. Austin, M. P. Chipperfield, F. Xie, and W. Wang, 2011: Effects of sea surface temperature and greenhouse gas changes on the transport between the stratosphere and troposphere. *J. Geophys. Res.*, **116**, D02124.
- Škerlak, B., M. Sprenger, and H. Wernli, 2014: A global climatology of stratosphere-troposphere exchange using the ERA-Interim data set from 1979 to 2011. *Atmos. Chem. Phys.*, **14**, 913–937.
- Solomon, S., J. S. Daniel, R. R. Neely, J. P. Vernier, E. G. Dutton, and L. Thomason, 2011: The persistently variable “background” stratospheric aerosol layer and global climate change. *Science*, **333**, 866–870.
- Sprenger, M., M. Croci Maspoli, and H. Wernli, 2003: Tropopause folds and cross-tropopause exchange: A global investigation based upon ECMWF analyses for the time period March 2000 to February 2001. *J. Geophys. Res.*, **108**, 8518.
- Stohl, A., and co-authors, 2003: Stratosphere-troposphere exchange: A review, and what we have learned from STAC-CATO. *J. Geophys. Res.*, **108**, 8516.
- Su, H., J. H. Jiang, X. Liu, J. E. Penner, W. G. Read, S. T. Massie, M. R. Schoeberl, P. Colarco, N. J. Livesey, and M. L. Santee, 2011: Observed increase of TTL temperature and water vapor in polluted clouds over Asia. *J. Climate*, **24**, 2728–2736.
- Sun, Y., and Y. Huang, 2015: An examination of convective moistening of the lower stratosphere using satellite data. *Earth Space Sci.*, **2**, 320–330.
- Textor, C., H. F. Graf, M. Herzog, and J. M. Oberhuber, 2003: Injection of gases into the stratosphere by explosive volcanic eruptions. *J. Geophys. Res.*, **108**, 4606.
- Vernier, J. P., L. W. Thomason, J. P. Pommereau, A. Bourassa, J. Pelon, A. Garnier, A. Hauchecorne, L. Blanot, C. Trepte, D. Degenstein, and F. Vargas, 2011: Major influence of tropical volcanic eruptions on the stratospheric aerosol layer during the last decade. *Geophys. Res. Lett.*, **38**, L12807.
- Wang, T., W. J. Randel, A. E. Dessler, M. R. Schoeberl, and D. E. Kinnison, 2014: Trajectory model simulations of ozone (O3) and carbon monoxide (CO) in the lower stratosphere. *Atmos. Chem. Phys.*, **14**, 7135–7147.
- Yan, R. C., and J. C. Bian, 2015: Tracing the boundary layer sources of carbon monoxide in the Asian summer monsoon anticyclone using WRF-Chem. *Adv. Atmos. Sci.*, **32**, 943–951.
- Zhan, R., and Y. Wang, 2012: Contribution of tropical cyclones to stratosphere-troposphere exchange over the northwest Pacific: Estimation based on AIRS satellite retrievals and ERA-Interim data. *J. Geophys. Res.*, **117**, D12112.